Influence of Electronic Resonances on Mode Selective Excitation with Tailored Laser Pulses

J. Konradi,[‡] A. Gaál,[§] A. Scaria,[‡] V. Namboodiri,[‡] and A. Materny[‡]*

School of Engineering and Science, Jacobs University Bremen,[†] Campus Ring 1, D−28759 Bremen, Germany, and Faculty of Mathematics, Physics and Informatics, Comenius University, Mlynská dolina, 842 48 Bratislava, Slovak Republic

Received: June 11, 2007; In Final Form: October 16, 2007

Femtosecond time-resolved coherent anti-Stokes Raman scattering (fs-CARS) gives access to ultrafast molecular dynamics. However, the gain of the temporal resolution entails a poor spectral resolution due to the inherent spectral width of the femtosecond excitation pulses. Modifications of the phase shape of one of the exciting pulses results in dramatic changes of the mode distribution reflected in coherent anti-Stokes Raman spectra. A feedback-controlled optimization of specific modes making use of phase and/or amplitude modulation of the pump laser pulse is applied to selectively influence the anti-Stokes signal spectrum. The optimization experiments are performed under electronically nonresonant and resonant conditions. The results are compared and the role of electronic resonances is analyzed. It can be clearly demonstrated that these resonances are of importance for a selective excitation by means of phase and amplitude modulation. The mode selective excitation under nonresonant conditions is determined mainly by the variation of the spectral phase of the laser pulse. Here, the modulation of the spectral amplitudes only has little influence on the mode ratios. In contrast to this, the phase as well as amplitude modulation contributes considerably to the control process under resonant conditions. A careful analysis of the experimental results reveals information about the mechanisms of the mode control, which partially involve molecular dynamics in the electronic states.

Introduction

The investigation of the elementary molecular dynamics following an excitation of complex systems is of considerable interest. A chemical reaction is determined by the breaking and forming of chemical bonds resulting from energy flow within the molecule. Theses fundamental processes are occurring on the ultrashort time scale of molecular vibrations. Raman spectroscopy yields information about the vibrational and rotational modes of molecules with high-frequency resolution. However, the dynamics in most cases is not accessible in frequency domain spectroscopy. The application of femtosecond laser pulses allows for a direct observation of molecular dynamics[1−3] on ultrashort time scale. Different time-resolved spectroscopical techniques used to get insight into dynamical aspects of photochemical reactions were developed recently. Since the high powers of femtosecond laser pulses favor nonlinear optical processes, also the higher order nonlinear spectroscopical techniques like four wave mixing (FWM) are widely used. In particular, coherent anti-Stokes Raman scattering (CARS)[4−12] is a widely used FWM technique for the study of the vibrational motion in a molecule, where the molecule is prepared by two coherent lasers and probed by another laser. Using femtosecond laser pulses, the vibrational dynamics in ground as well as excited electronic states are accessible.[6] However, the gain of temporal resolution entails a poor spectral resolution due to the inherent spectral width of the femtosecond excitation pulses.[1,2] Since several molecular states (e.g., vibrational modes) falling within the broad spectrum of the laser pulses are excited coherently,[6,10] the detected signal results from a coherent superposition of several excited modes.[2,3] The analysis of a particular mode in a polyatomic molecule is often complicated due to the contributions arising from other vibrational modes of the molecule. Hence, a technique, which helps to filter out the contributions from unwanted modes and to enhance the signal obtained from a specific vibrational state would be of great interest.

A promising approach for mode-selective excitation even in complex systems is the application of coherent control.[13−19] Using this technique, the molecular dynamics are guided with specifically designed light fields.[13,14,16] The wide spectra of femtosecond laser pulses are manipulated by a pulse shaper device[20] to generate an electric field profile adapted to the desired result. The coherence properties of the laser field are exploited to achieve constructive interference for desired states or reaction channels via a phase correct superposition of wave functions. Recent works of the groups of Gerber[21−26] and Silberberg[27−31] illustrate several fundamental and practical aspects of coherent control in gas as well as liquid phase. In an earlier publication we have reported also the drastically changed femtosecond CARS spectra and transients obtained from single crystals of polydiacetylene (PDA)[10] due to slight variations of the chirps of pump and/or Stokes laser pulses. Consequently, it seems to be possible to "focus" the excitation on one or more selected vibrational modes using suitable shaped laser pulses or pulse sequence.

The electric field required for such mode-selective excitation can be predicted by optimal control theory[14] starting from the Hamiltonian of the molecular system. However, this approach is restricted to simple molecules only and does not take into account the experimental limitations. An alternative to find the optimal laser field also for more complicated molecules is the

* Author to whom correspondence should be addressed. E-mail: a.materny@iu-bremen.de.
† Formerly International University Bremen.
‡ School of Engineering and Science, Jacobs University Bremen.
§ Faculty of Mathematics, Physics and Informatics, Comenius University.

10.1021/jp0745079 CCC: $40.75
Published on Web 01/29/2008

use of a self-learning loop approach as suggested by Judson and Rabitz.[16] Here, the search of the optimal control field is guided by an optimization algorithm, which employs the direct feedback from the experimental output and controls the pulse shaper device. Experimentally, the optimization algorithm can be realized by applying evolutionary strategies, which use the feedback signal as a fitness function measuring the success of the optimization.[32] Since the experimental response of the molecule is directly interrogated, a prior knowledge of the molecular Hamiltonian is not required. The electronic and vibrational properties of the molecular system as well as necessary corrections to the experimental conditions are all "taken into consideration" by the feedback-controlled optimization. Adaptive control was first reported by Wilson et al.[33] Here, by shaping the femtosecond pulses, the fluorescence signal from a dye molecule could be maximized.

Recently, we have presented the results obtained from mode-selective excitation in femtosecond CARS spectrum[34−37] performed on various molecular systems by means of a pure phase modulation of the Stokes pulse. In all cases, we have observed drastic changes of the CARS spectra resulting from the optimization. E.g., in mixtures of different molecules, the selected vibrational modes could be excited exclusively, i.e., the contribution from a molecular component in the mixture could be enhanced relatively while the modes of the other component were suppressed. The "focusing" of the excitation occurred for the complete coherence lifetime of the time dependent CARS signal.

While in our former experiments the spectral phases of the exciting laser pulses, exclusively, were modulated, the present contribution reports the influence of an additional degree of freedom. In our recent complementary experiments,[38] we also have varied the amplitudes of the spectral components. In order to demonstrate the role of the electronic transition on the control process in the following, we discuss the results of experiments performed on toluene under nonresonant[38] conditions and on crystal violet under resonant conditions. The feedback-controlled optimization was carried out by modulating the spectral phases and amplitudes laser pulses exclusively or in combination. We will demonstrate that for the mode control in the nonresonant case, the complete spectrum of the pulse is required and hence amplitude modulation does not improve the result. However, when dynamics on an excited potential energy surface is involved, the selection of certain spectral components is of great importance for the success of the optimization. Here, not only relative changes of the mode contributions to the CARS spectra could be observed, but also absolute enhancements of the optimized nonlinear Raman lines. Like in our former experiments, in many cases only very small changes of the pulse shapes resulted in drastic spectral changes.

Theory

Femtosecond coherent anti-Stokes Raman scattering (CARS) is a four-wave mixing (FWM) process induced by the nonlinear interaction of three ultrashort laser pulses with the sample molecules. The first two pulses having frequencies ω_{pu} and ω_S are labeled as pump and Stokes pulses, respectively. Their nonlinear interaction induces a second-order polarization resulting in the coherent excitation of vibrational modes in the ground electronic state. The frequency difference $\Omega = \omega_{pu} - \omega_S$ corresponds to the frequency of the vibrational states excited by the stimulated Raman process. Owing to the broad spectral bandwidth of the femtosecond pulses, several molecular vibrational modes are excited simultaneously. The third pulse acts as the probe pulse and has a frequency ω_{pr}, which in our experiments was chosen to be equal to ω_{pu}. The probe laser interacts with the coherently excited vibrational states to create a third-order polarization. The anti-Stokes signal arising from this nonlinear interaction is coherent and directed. The direction of CARS signal is determined by the phase matching condition resulting from momentum conservation. A variation of the time delay between the exciting and probing pulses, gives access to information about coherent dynamics taking place in the excited molecules. The excitation of vibrational modes may occur resonantly via excited electronic states as well as nonresonantly without the involvement of electronic transitions. For an electronically resonant excitation the frequencies of pump and probe lasers are tuned to the electronic transition of the molecular system, which results in a considerable enhancement of the signal intensity.

The nonlinear interaction of pump $\tilde{\mathbf{E}}_{pu}$, Stokes $\tilde{\mathbf{E}}_S$, and probe $\tilde{\mathbf{E}}_{pr}$ pulses is described by the complete expression of third-order polarization[39] in the time domain. In the model introduced in the following,[30,40] the third-order polarization in the frequency domain is described by a separation into nonresonant and resonant contributions. The nonresonant background is caused by the instantaneous electronic response of the molecular sample and lasts for the duration of the cross-correlation time of the pump and Stokes pulses. The resonant CARS signal reflects the vibrational structure of the molecule. For the nonresonant contribution it is assumed that all intermediate states are far from resonance. The third-order polarization is then approximated by

$$P_{nr}^{(3)}(\omega) \propto \int_0^\infty d\Omega\, \mathbf{E}_{pr}(\omega - \Omega) \int_0^\infty d\omega_1\, \mathbf{E}_s^*(\omega_1 - \Omega)\mathbf{E}_{pu}(\omega_1) \quad (1)$$

For a singly resonant Raman transition via the intermediate level $|i\rangle$ the nonlinear polarization is given by the expression:

$$P_r^{(3)}(\omega) \propto \int_0^\infty d\Omega\, \frac{\mathbf{E}_{pr}(\omega - \Omega)}{(\omega_R - \Omega) + i\Gamma} \int_0^\infty d\omega_1\, \mathbf{E}_S^*(\omega_1 - \Omega)\, \mathbf{E}_{pu}(\omega_1) \quad (2)$$

where ω_R is the resonance frequency and Γ is the bandwidth of the Raman line. The integral term of the complex field amplitudes included in both expressions describes the second-order polarization responsible for the excitation of the molecular vibrations. This convolution integral of $\mathbf{E}_S(\omega)$ and $\mathbf{E}_{pu}(\omega)$ yields the excitation amplitude for a certain Raman mode induced by the nonlinear interaction of pump and Stokes pulses having a frequency difference of Ω:

$$A(\Omega) = \int_0^\infty d\omega_1\, \mathbf{E}_S^*(\omega_1 - \Omega)\, \mathbf{E}_{pu}(\omega_1) \quad (3)$$

In the time-domain the second-order polarization of the stimulated Raman excitation is given by the product of the real electric fields of the pump and Stokes pulses, $\tilde{\mathbf{E}}_{pu}(t)$ and $\tilde{\mathbf{E}}_S(t)$, respectively:

$$\tilde{A}(t) = \mathbf{F}^{-1}(A(\Omega)) = \tilde{\mathbf{E}}_S(t)\tilde{\mathbf{E}}_{pu}(t) \quad (4)$$

Taking into account the time-delay $\Delta\tau_1$ between pump and Stokes pulses, the excitation of the Raman mode with the stimulated Raman frequency Ω is given by the Fourier transform of the product of the electric fields in the time-domain:

$$A(\Omega, \Delta\tau_1) = \mathbf{F}(\tilde{\mathbf{E}}_{pu}(t)\tilde{\mathbf{E}}_S(t + \Delta\tau_1)) \quad (5)$$

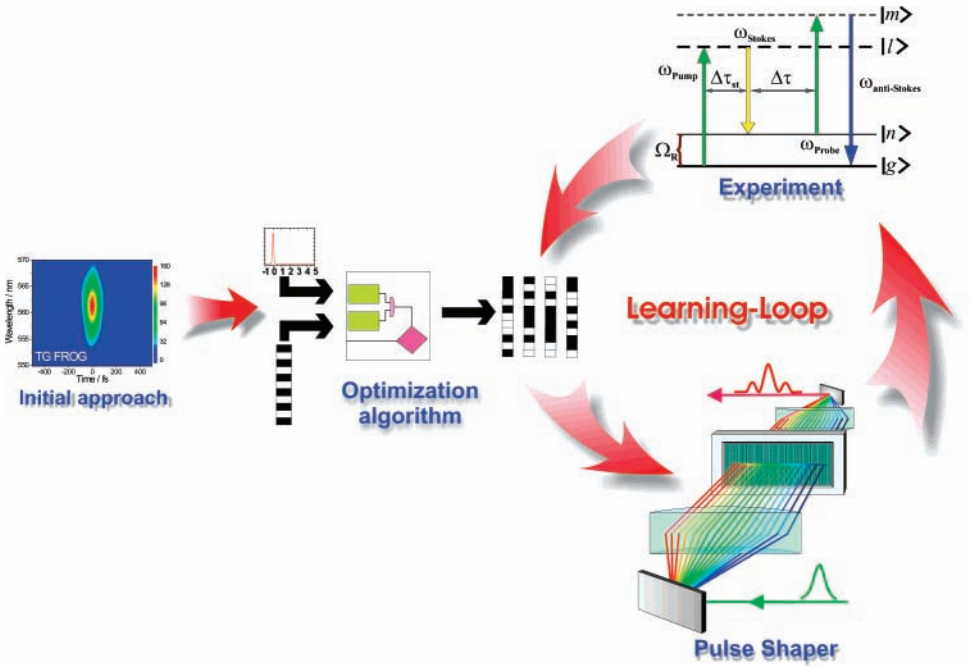

Figure 1. Optimal control setup: Schematic representation of the feedback-controlled optimization experiment. Starting with an initial guess, the optimization algorithm realized by evolutionary strategies controls the settings of a liquid crystal spatial light modulator(LC SLM) placed in the Fourier plane of a 4*f* zero-dispersive grating arrangement. The shaped pulses are used for the coherent anti-Stokes Raman scattering (CARS) experiment and the ratio of certain Raman line intensities in the resulting spectrum serves as fitness function for the optimization algorithm. On the basis of the feedback signal, the control software proposes new phase mask parameters in order to find the extremum of the fitness function.

Analogously, the third-order polarization in the frequency domain is given by the Fourier transform of the product of the electrical fields of pump, Stokes, and probe pulses in the time-domain:

$$P_{\mathrm{nr}}^{(3)}(\omega, \Delta\tau_1, \Delta\tau_3) = \mathbf{F}(\tilde{\mathbf{E}}_{\mathrm{pr}}(t+\Delta\tau_2)\tilde{\mathbf{E}}_{\mathrm{pu}}(t)\tilde{\mathbf{E}}_{\mathrm{S}}(t+\Delta\tau_1)) \quad (6)$$

Using this expression the complete CARS spectrum can be calculated in the time-domain, taking into account the delay between pump and Stokes pulses as well as that between probe pulse and stimulated Raman excitation.

Experimental Section

The investigations were performed on liquid toluene and on an aqueous solution of crystal violet (CV). The samples were obtained from Aldrich and used as received. The toluene filled in 2 mm thin quartz cell was used without further purification. The CV was diluted in distilled water. The resulting CV solution, having a concentration of $\approx 5 \times 10^{-5}$ M, was used in a quartz cell with cell length of 1 mm.

Figure 1 shows a schematic presentation of the optimal control setup based on a feedback-controlled self-learning loop. The three basic components are the creation and shaping of the femtosecond laser pulse, the experimental setup for time-resolved CARS spectroscopy, and the optimization algorithm, which is linked to the other two components. As a source for the three femtosecond laser pulses required for the four-wave mixing (FWM) experiment we have employed two optical parametrical amplifiers (OPA; Light Conversion, TOPAS) pumped by a commercial Ti:sapphire laser system (Clark-MXR Inc., CPA-2010, 1 kHz repetition rate). The output beam from one OPA was compressed to approximately 80 fs with a pair of prisms and served as Stokes pulse. The output of the other OPA was split into two equal parts by a beam splitter to create pump and probe pulses. After the compression by a prism arrangement, the resulting temporal width of the probe pulse was in the range between 85 and 95 fs. The pump pulse was spectrally phase and amplitude modulated by the pulse shaper device.[20,41] In the pulse shaper, the input pulse was dispersed into its spectral components by a combination of a grating (1800 l/mm) and a cylindrical mirror (focal length $f = 300$ mm). A second pair of identical grating and mirror recombined the pulse spectrum in a zero-dispersion compressor setup. The first cylindrical mirror forms an image of the spectrum parallel onto the Fourier plane, the second focuses it onto the second grating. A liquid crystal (LC) spatial light modulator (SLM-S640d, Jenoptik)[42] placed in the Fourier plane of the setup modulated the spectral features of the pulse. The phase and/or amplitude of certain spectral components could be varied by applying suitable voltages to the 640 individual stripes.[43] The compressed Stokes and probe pulses, and the shaped pump pulse were applied for the CARS experiments. The phase matching condition was fulfill in a folded BoxCARS configuration.[44] Here, the excitation beams were arranged in the three edges of a square perpendicular to the optical axes of the parallel beams. Lenses with focal lengths of 100 mm focused the lasers into the sample respectively made the transmitted laser beams together with the anti-Stokes signal parallel again. The anti-Stokes signal appeared in the fourth edge of the square and was well spatially separated from the laser beams. The laser background was suppressed by using a pinhole for the CARS signal, which was detected spectrally resolved using a single monochromator (TRIAX 180, HORIBA Jobin Yvon) and a peltier-cooled CCD camera.

In the experiments discussed in the following section, we have applied an evolutionary algorithm[32] to control the optimization process. For this, 64 different pulse shapes were used for each generation. Each of these individuals is represented by a set of free parameters, which determine the modulation of the shaped pulses. How many and which parameters were varied during the optimization depended on the modulation function and on whether phase and/or amplitude modulation were applied to the

pulse spectrum. The eight best individuals were used to create a new generation by crossover. Four of these individuals were changed by mutation. In general, convergence could be achieved after only few loops. Therefore, in most cases, the number of loops could be limited to approximately 10 generations. As a feedback signal for the optimization of a specific mode contribution, the relative intensities of the vibrational modes covered by the CARS excitation were used.

Before starting the experiments, the pump pulse was compressed by means of pure phase modulation. The intensity of a second harmonic generation (SHG) generated by the pump pulse in a BBO crystal served as fitness function for this optimization. The compressed pump and Stokes pulses were overlapped temporally and then fixed. Relative temporal shifts due to the phase shaping are part of the control and therefore not compensated (see below). The frequency difference between pump and Stokes pulse determines which modes are excited coherently. The probe pulse monitors this mode excitation at variable time delay. In order to avoid the nonresonant contribution to the CARS spectrum at zero time, a fixed delay time between probe pulse and stimulated Raman excitation was introduced. The optimization and the recording of the resulting spectra were performed at 1.2 ps probe time delay for the investigation on toluene and at 900 fs for CV. The time-resolved CARS spectra were recorded before and after optimization by scanning the time delay of the probe pulse relative to the pump and Stokes pulse pair.

The results presented in the following were obtained from the optimization using phase and/or amplitude modulation of the pump pulse. The phase function applied on pump pulse was simplified by a polynomial representation as described below:[34]

$$\Phi_n = \sum_{k=2}^{K} c_k \left(\frac{n - N_0}{N} \right)^k \quad \text{with } n = 0, ..., N-1 = 639 \tag{7}$$

This polynomial of order K determined by the coefficients c_k specifies a phase value for each liquid crystal (LC) stripe. The variables N and n describe the number of LC stripes and the individual stripe, respectively. Since the linear term with $k = 1$ results in a pure temporal shift of the shaped pump pulse, we have omitted this order. The lowest polynomial order is represented by the quadratic term. The parameter N_0 is the offset of the phase function, which determines the spectral component with unchanged phase. Initially, the offset coincides with the center of the spectrum on the LCD. The variation of this parameter introduces also a linear phase shift and consequently a temporal shift of the pulse. In our experiments, a fifth order polynomial was used to describe the modulation of the phase of the pump pulses. For the amplitude modulation of the pump pulse we have tested different mathematical functions (free optimization of stripes, polynomial, Gaussian, etc.). The best results were obtained by using a rectangular or Gaussian function for the transmission and blocking of specific parts of the pulse spectrum. In the following we will restrict our discussion to results obtained from such amplitude functions. The offset N_0, and four coefficients c_k for the phase, the central position, and the width of the spectral windows served as fitting parameters for the optimization guided by the evolutionary algorithm.

The pulse shapes obtained from the optimizations were analyzed by means of the frequency-resolved optical gating (FROG) technique.[45] The home-built FROG device used in our experiments is based on a transient-grating (TG) FWM configuration. Here, the input pulse is split into three beams of equal intensity. These beams are arranged in a folded BoxCARS geometry and focused into a thin sapphire plate. The resulting TG signal was detected by a spectrometer equipped with a CCD camera and the spectra were recorded with respect to the delay of one of the beams. The resulting FROG traces were evaluated using the commercial software FROG 3.0.9 (Femtosoft Technologies) and yield the information about spectral phase and amplitude as well as the electrical field of the pulse.

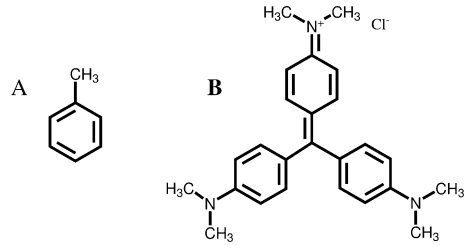

Figure 2. Molecular structures of toluene (A) and crystal violet (B).

Results and Discussion

The results discussed in the following were obtained from the application of the optimal control scheme for mode selective excitation described above. As mentioned earlier, the spectrally broad femtosecond laser pulses excite several vibrational modes simultaneously. The nonlinear character of the coherent anti-Stokes Raman excitation causes the relative enhancement of lines, which are strong in the linear Raman spectrum and relative suppression of weak contributions. The optimization of specific modes was performed by optimizing line ratios. That means that not the absolute line intensities were maximized. Therefore, if we talk about "enhancement" or "suppression" of modes in the following, we usually refer (if not explicitly mentioned otherwise) to the relative line intensities. The pulses were shaped by means of phase and/or amplitude modulation. The contributions of the two different modulations will be compared to learn more about their role in the optimization process. Also, the excitation of the CARS process was performed on molecular systems, where the femtosecond laser pulses were in resonance with an electronic transition. The comparison of these results helps to better understand the role of electronic resonances for the control process.

The molecular model systems considered in the following are liquid toluene and an aqueous solution of crystal violet (CV). Their vibrational spectra are characterized by several strong well separated lines within the bandwidth of the excitation. The assignment of these Raman active modes is well-known.[46,47] The molecular structures of toluene and CV are given in Figure 2. Toluene (panel A of Figure 2) is absorbing in the UV spectral region. Therefore, the pulse wavelengths applied in the CARS experiments are not in resonance with an electronic transition. For the electronically nonresonant excitation the central wavelength for pump and pulses was tuned to 562 nm. The Stokes laser was set to 593 nm resulting in a Raman excitation at a wavenumber difference of 950 cm^{-1} between pump and Stokes lasers. Both laser wavelengths are far off resonance with the UV absorption. CV is a nonplanar molecule (panel B of Figure 2) and is characterized by three phenyl rings forming a propeller-like structure twisted with respect to each other. The absorption of CV is in the visible spectral range having its maximum at 590 nm. The wavelengths of the pump and probe pulses applied for the control experiment on CV were tuned to resonance with the electronic transition from ground to first excited state. Selecting a central wavelength of 592 nm for pump and probe

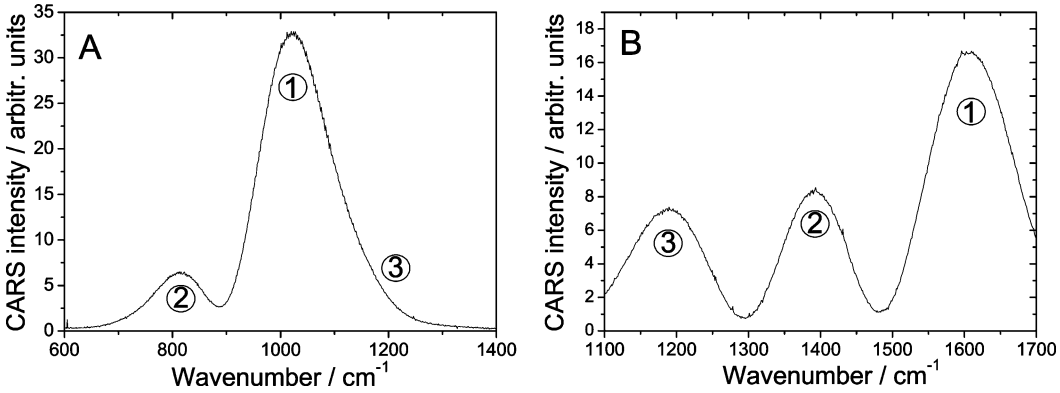

Figure 3. Femtosecond CARS spectra of liquid toluene (A) and aqueous solution of crystal violet (B). The spectrum in panel A is recorded under electronically nonresonant conditions using pump and probe pulses spectrally centered at 562 nm and Stokes pulse at 593 nm. For the CARS spectrum in panel B, electronically resonant conditions were chosen using a central wavelength of 592 nm for the Stokes pulse.

pulses and 642.5 nm for the Stokes pulse resulted in a stimulated Raman excitation centered spectrally at approximately 1350 cm^{-1}.

The starting point for our investigation are the femtosecond CARS spectra taken with compressed pulses. The initial CARS spectra of toluene and CV are shown in panels A and B of Figure 3, respectively. In agreement with our earlier results[35,38] this spectrum is characterized by a dominant mode at 1000 cm^{-1} in the following referred to as band ①. Band ② at 800 cm^{-1} was observed in our previous experiments[35] only as a shoulder red-shifted by 200 cm^{-1} relatively to band ①. We have shifted the resonance of the stimulated Raman excitation to further enhance band ②. The blue-shifted shoulder observed previously[35,38] at approximately 1200 cm^{-1} (band ③) can only be seen here as an asymmetry in the line shape of band ①. The reason for this choice of pump-Stokes wavelength difference is explained below. The nonoptimized spectrum of CV shown in panel B of Figure 3 is characterized by three well separated bands. In the following, the strong peak at 1600 cm^{-1} is referred to as band ①. It arises from the unresolved contributions of the Raman modes at 1537, 1589, and 1622 cm^{-1}.[47] The simultaneous excitation of the vibrational modes at 1371, 1390, 1443, and 1484 cm^{-1} results in a broad band at approximately 1400 cm^{-1}, labeled as band ②. And finally, the band ③ of the CV CARS spectrum observed at approximately 1200 cm^{-1} corresponds to the molecular vibrations having wavenumbers 1177 and 1299 cm^{-1}.

Mode-Selective Excitation under Nonresonant Conditions. We begin our systematic study by analyzing the optimization results for the Raman lines of liquid toluene. Previously, we have demonstrated the selective excitation of the vibrational bands ①, ②, and ③ in the CARS spectrum of toluene.[35,38] There, high efficiency of the optimization was achieved by means of pure phase modulation of the Stokes laser pulse. The wavenumber difference between the pump and Stokes pulse was tuned to the Raman resonances at approximately 1060 cm^{-1}. The experiments presented in the following were investigating the influence of the pump laser pulse shape on the CARS spectra. We started with the same stimulated Raman excitation wavenumber, 1060 cm^{-1}, which in contrast to the CARS spectrum shown in panel B of Figure 3A also resulted in a well-separated band ③ contribution. The efficiency of the control was found to be extremely small. In particular, for band ③ a relative enhancement only could be observed when the overall intensity of the CARS spectrum was drastically reduced. Since reasonable control results could only be obtained from experiments trying to optimize bands ① or ②, we decided to shift the Raman excitation to a center wavenumber of 950 cm^{-1} as already mentioned earlier. Under these conditions band ③ nearly vanishes. Nevertheless, in the following we will also give the intensity values for band ③ for the sake of completeness.

The optimization results are presented in Figure 4. The fitness functions used by the evolutionary algorithm were measuring the intensity ratios of the bands. Again, while the optimizations worked for bands ① and ②, a relative enhancement of band ③ could not be achieved. However, the efficiency of the control by pump pulse shaping was clearly less than that observed earlier for Stokes pulse modulation. As will be obvious from the experimental results discussed in the following, the efficiency of the control by phase modulation of the pulse decreases if the bandwidth of the pulse is reduced. This is in accordance with results reported previously[38] and could in principle explain the reduced efficiency for the mode excitation control by shaping the pump pulse if the pump pulse would be spectrally narrower than the Stokes pulse. However, both a slight shift of the central wavelength of the pump pulse and an increase of its bandwidth could not significantly improve the efficiency of the control process. Up to now, we have no plausible explanation for the different role of pump and Stokes laser pulses in the nonresonant case. Theoretical work is in progress; however, it has proven to be very demanding.

The graphs on the left-hand side of Figure 4 show the femtosecond CARS spectra optimized for band ① (panels C, E, and G) and for band ② (panels B, D, and F). Spectrum A, recorded with a transform limited pump pulse, is given for comparison. The pump pulses resulting from the optimization were analyzed using the TG FROG. The corresponding spectrograms are given in the respective panels (A−G) on the right-hand side of Figure 4. All optimized spectra are characterized by a drastically reduced intensity of the overall signal relative to the initial spectrum shown in panel A. The numbers in the brackets above the different bands indicate the intensities of these modes relative to the intensity of band ① obtained from the measurement with transform limited pump pulse, which was set to unity. Panels B and C show the results of a mode selective excitation by pure phase modulation. Spectrum C, optimized for band ①, is characterized by a complete suppression of band ②. The mode selective excitation of band yields a drastic reduction of band ①, as shown in spectrum B. The selected band is dominating the spectrum. However, in contrast to earlier results,[35] band ① was not completely suppressed. As already discussed above, for the electronically nonresonant stimulated Raman process, the pump laser modulation was less efficient for the selective excitation of modes than the shaping of the Stokes laser pulse. The pump pulses resulting in spectra B and C are characterized by a negative linear chirp with nonlinear

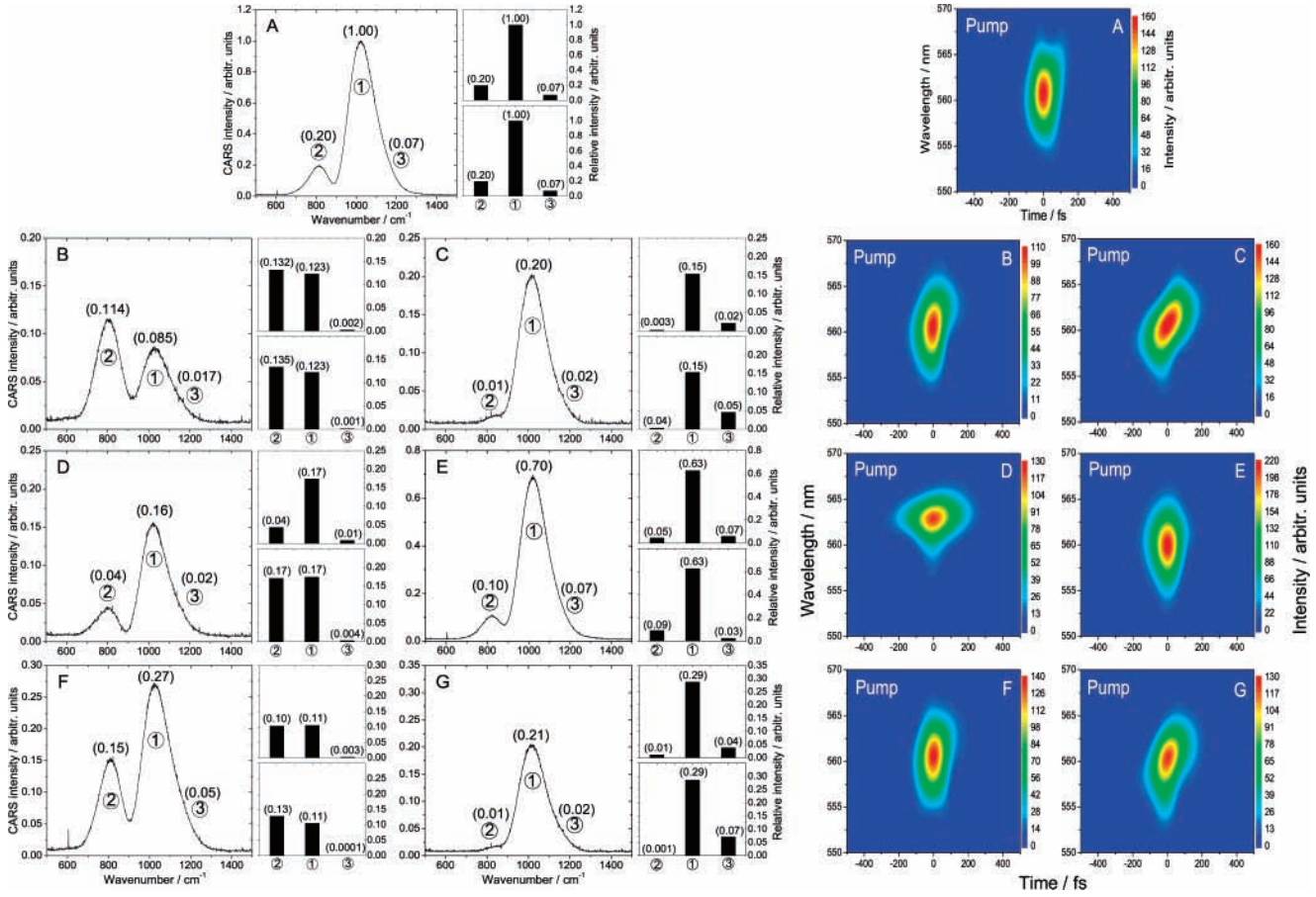

Figure 4. Optimization results in a control experiment on liquid toluene, where the pure spectral phase (B−C), pure spectral amplitude (D and E), and both spectral phase and amplitude (F−G) of the pump pulse were modulated. The graphs on the left-hand side show the spectra obtained from the optimization, recorded at 1200 fs time delay of the probe laser pulse. The numbers in brackets above the different bands indicate their intensities using equal scales for each panel. Panel A shows the spectrum taken with transform-limited pulses for comparison. Panels B, D, and F show the spectra optimized for band ②. The spectra in panels C, E, and G are optimized for band ①. The bar diagrams on the right-hand side of the each spectrum show the line intensities predicted from the nonresonant CARS spectrum taken from a thin glass plate (upper diagrams) and obtained from a calculation (bottom diagrams), which used the electric fields of the pulses derived from the FROG traces. The intensity of band ① in panel A is normalized. The corresponding spectrograms are shown in the respective panels A−G on the right-hand side.

components. Their temporal widths are approximately 110 and 160 fs, respectively. The femtosecond CARS spectra shown in panels D and E are obtained from the optimization by pure amplitude modulation. Only slight changes in the optimized spectra relative to spectrum A obtained before pulse shaping are observed. The optimized pulse shapes are clearly modified compared to the initial pulse. The pulse spectrum is narrowed and the spectral intensity maxima are shifted relative to the original pump center wavelength toward a position close to a wavenumber difference of pump and Stokes in resonance with the selected band. While the optimizations by means of pure phase modulation result in clearly changed CARS spectra, the ratio of the Raman line intensities is only slightly varied by amplitude-only modulated pump pulses. The involvement of a spectral phase modulation as control parameter seems to be required for an efficient excitation of selected vibrational modes under electronically nonresonant conditions. In order to confirm this observation, an optimization with both phase and amplitude modulation was used to excite band ② or ① selectively. The resulting spectra are shown in panels F and G. One would expect an even better optimization result compared to the phase-only and amplitude-only modulation experiments. However, the additional degree of freedom even decreased the optimization efficiency. As already observed earlier,[37,38] any reduction of the pulse spectrum results in a limitation of the ability to influence the mode excitation by pulse shaping. Additionally, from a certain point on a further increase of the number of parameters varied by the evolutionary algorithm (e.g., higher order polynomial) makes it more difficult for the program to find the optimal result. This was already observed during our earlier experiments. The optimizations achieved by the combined phase and amplitude modulation resulted in pump pulse shapes (see corresponding FROG traces), which show a clear similarity to the phase-only optimized pulses. This points to the major contribution of phase modulation to the mode selective excitation.

In literature different mechanisms are discussed, which are capable of influencing the mode excitation. (i) Weiner et al.[48,49] have demonstrated the application of an "impulsive stimulated Raman excitation" for the selective excitation of vibrational modes. This technique utilizes a sequence of pulses in order to resonantly drive a selected mode if the frequency of the pulse sequence is equal to the vibrational frequency of the respective mode.[50−52] None of shaped pulses shown in Figure 4, which were obtained from the optimization shows such a pulse structure. The impulsive stimulated Raman process does therefore not have to be considered as mechanism for the spectrum control performed by feedback-controlled optimization as long as pulse sequences are not enforced by certain pulse modulation functions. (ii) Another possibility to excite vibrational modes selectively was reported by Silberberg and co-workers.[28−31] These authors have successfully applied a phase modulation on the exciting pulses to enhance selected vibrational modes and

to suppress nonresonant background in a CARS spectrum. Using a pulse shaper setup equipped with an LCD, rectangular[29,31] or steplike[30] π phase shifts were introduced to both pump and Stokes pulses or to the probe pulse. This method makes use of the fact that a driven oscillator if excited off resonance is out of phase with its driving field by $\pm\pi/2$. The adjustment of the phase step position to the resonance frequency of the vibration utilizes the off-resonant part of the spectrum to enhance the selected mode contribution. The pulses resulting from our optimization attempts in no case show phase steps, which would explain a mode enhancement as described by Silberberg's group. (iii) The third and perhaps simplest and most straightforward mechanism was recently demonstrated by Zumbusch and coworkers.[53] In their experiments, they used a Fourier-transform limited pump and a linearly chirped Stokes pulse. The time delay between these pulses and consequently their spectral overlap were varied. This results in a shift of the wavenumber difference of the pulses and such in a change of the stimulated Raman excitation resonance. Also in our experiments, the variation of the optimization parameter N_0, in particular, results in a temporal shift of the shaped pump pulse relative to the transform limited Stokes pulse. It could therefore be that the observed variation of line intensity ratios is due to this trivial shift of excitation wavenumbers. Such a shift would even more efficiently be achieved by an appropriate change of the pulse spectrum by means of an amplitude modulation.

In order to find out to what extent the simple "excitation shift mechanism" (ESM) due to phase modulation and the "spectral selection mechanism" (SSM) due to amplitude modulation contribute to our optimization results, additional experiments as well as a theoretical approach are used. Both methods provide comparable results as was already shown earlier.[37] To characterize the spectral overlap of the shaped and unshaped laser pulses experimentally, the pulses were before and after optimization also used to record (electronically and vibrationally) nonresonant CARS spectra from a thin glass plate. Since here the laser pulses interact with the glass medium without any electronic or Raman resonances, the resulting nonresonant anti-Stokes signal directly gives the cross-correlation and such also any possible influence of ESM or SSM. On the basis of these nonresonant CARS spectra, we have calculated the expected intensities at the wavenumber positions of the Raman modes under consideration. From this the prediction of enhancement or suppression of a mode due to ESM or SSM should be possible, if these mechanisms really determine the outcome of the optimization experiment. Additionally, a simple theoretical approach was used to estimate the influence of ESM and SSM. For a calculation of the expected (nonresonant) CARS spectrum by eq 6 the electrical fields of the pulses gained from the FROG traces were employed. Also here, a change of line intensities due to a different excitation via ESM or SSM should be detectable. However, the calculations based on the FROG traces proved to be less precise if the pulse spectra became too narrow. Therefore, in general, the experimentally obtained cross-correlations are more reliable.

In our earlier work,[37] we have investigated the importance of optimization parameters on the control process. We could demonstrate, that the observed resonant CARS spectral changes can completely deviate from the predictions made according to the ESM (phase-only modulation). This pointed to a nontrivial mechanism involving the molecular dynamics, which was driven by the shaped laser pulses into the desired direction.

The bar diagrams on the right-hand side of each CARS spectrum in Figure 4 show the relative Raman line intensities as predicted from the experimentally (top) and theoretically (bottom) obtained nonresonant spectra. The line intensity of band ① in the spectrum taken with a transform limited pump pulse was normalized. All other bars are giving the predicted line intensities relative to this normalized band. The changes in excitation intensity obtained from the vibrationally nonresonant spectra were applied to the Raman line intensities obtained for a Fourier transform limited pump pulse (panel A) yielding the predicted CARS spectra. Since the theoretical model based on eq 6 yields no information about the absolute intensity of the anti-Stokes signal, the associated bar diagrams were scaled such that the intensities of band ① always are equal to the experimentally obtained bar diagram value obtained for the same pulse shape. Except for the results shown in panel D, the predicted line intensities taken from the experimentally obtained nonresonant glass spectra (upper diagrams) and those obtained from the calculations using the measured pulse shapes (bottom diagrams) are in good agreement. The spectrum in panel D was obtained by pure amplitude modulation. The resulting pump pulse has a considerably reduced spectral width. As mentioned above, the quality of the calculation decreases in such cases, which might be an explanation for the deviation of the theoretical predicted band ② intensity from that one obtained from the experimental approach. Both the relative and absolute intensity values from the bar diagrams are very close to the intensities seen in the CARS spectra obtained from the toluene control experiments. This points to a domination of ESM and SSM in the mode excitation process. As mentioned above, the results of our earlier experiments, where the control was achieved by a shaping of the Stokes laser pulse, could only be explained by assuming a direct influence on the ground state dynamics. Obviously, the pump laser only influences the mode excitation by a variation of the Raman resonant excitation due to its spectral changes.

Using the pump pulses optimized for specific vibrational modes, we also recorded the CARS spectra of toluene as a function of the probe pulse delay. The results are displayed in Figure 5. The experimental data shown in the different panels refer to the CARS spectra in the respective panels of 4. The transients shown in panel A of Figure 5 were recorded with the transform limited pump pulse. Here and in following, the time-dependent intensity of the anti-Stokes signal was recorded at the spectral positions of bands ①, ②, and ③. Panels B and C show the results obtained with phase-only modulated pulses. The application of amplitude only modulated pulses yields the transients in panels D and E. All transients are characterized by clear beating structures, which result from the quantum beating of molecular modes coherently excited by the femtosecond laser pulses.[5,6,11] The fast Fourier transformation (FFT) spectra on the right-hand side yield information about the modes, which contribute to the beating structure in the respective transients. The assignment of the beating frequencies observed in the FFT spectra is summarized in Table 1 and was already discussed in detail in refs 6 and 35. As observed in our earlier work,[35] the optimization of certain vibrational modes is also reflected in the beating structure. If a certain vibrational mode in the CARS spectrum is suppressed, the beating with this mode completely vanishes or is clearly reduced. The transients show that a relative suppression or enhancement of modes persists over the full coherence life time of the CARS signal. This is in perfect agreement with our earlier observations reported for electronically nonresonant[35,38] and resonant[34] excitation. The changes observed in the FFT spectra for pure amplitude modulation are smaller than those obtained from phase-only optimizations.

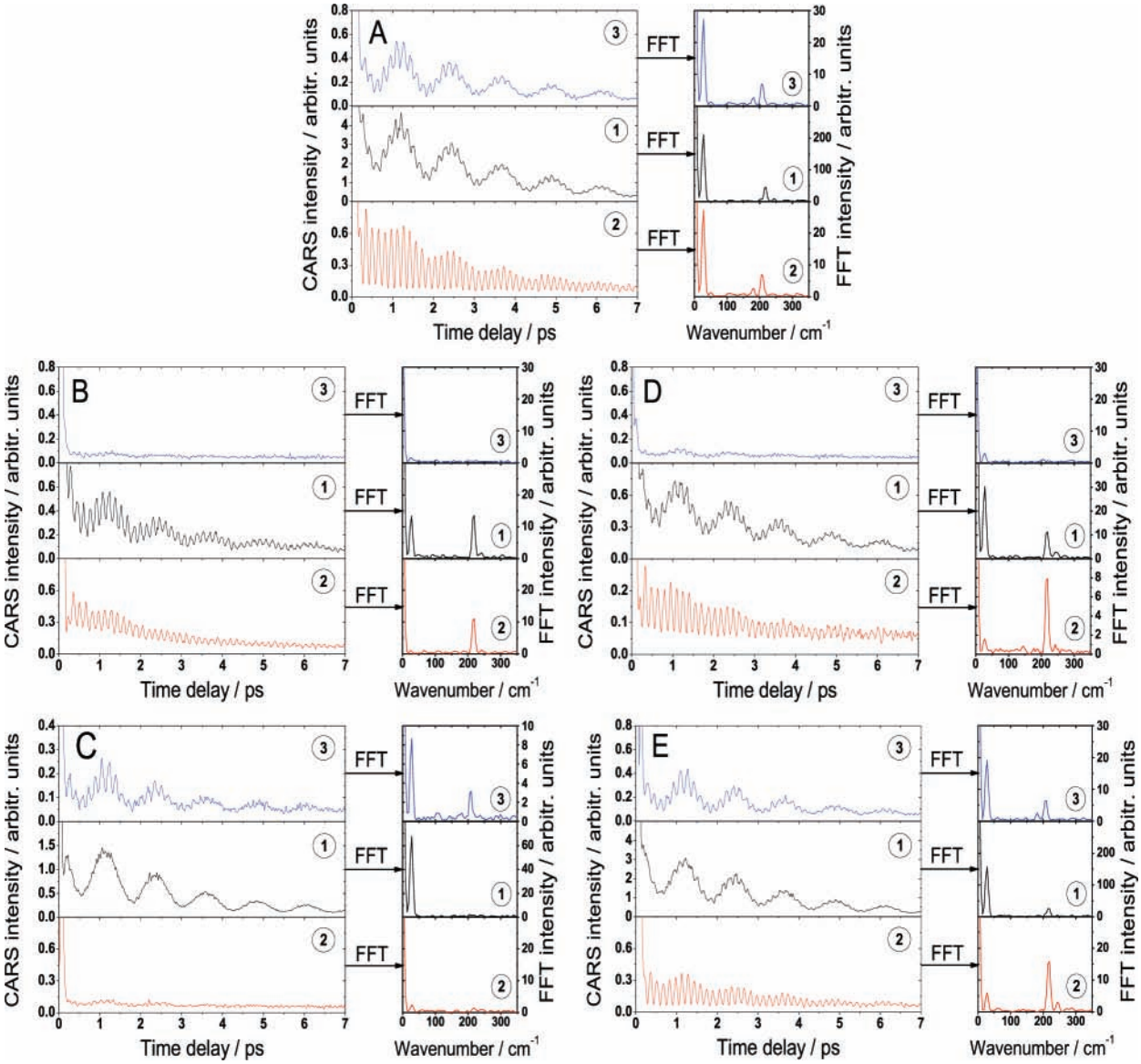

Figure 5. Transients obtained from the femtosecond time-resolved CARS experiments on toluene using the pump pulses described by their spectrograms in panels A−E on the right-hand side of Figure 4. The CARS transients were recorded by scanning the time delay between the temporally overlapped pump and Stokes pulses and the probe laser pulse. The time-dependent CARS signals are given at the spectral position of bands ①, ②, and ③. A fast Fourier transformation (FFT) has been attached to the right of each transient. The beating peaks observed in the FFT spectra and their assignment to the contributing modes are summarized in Table 1.

TABLE 1. Transients Taken at the Wavenumber Positions of the Different Bands Show a Beating Structure[a]

beating modes	$\Delta\tilde{\nu}$/cm^{-1}	contributing to bands
alkyl and $\tilde{\nu}_{10a}$	25	②
$\tilde{\nu}_{12}$ and $\tilde{\nu}_{18a}$	25	①
C_6H_5C group and $\tilde{\nu}_{9a}$	30	③
C_6H_5C group and $\tilde{\nu}_{15}$	50	③
C_6H_5C group and $\tilde{\nu}_{18a}$	180	①, ③
$\tilde{\nu}_{12}$ and C_6H_5C group	205	①, ③
alkyl and $\tilde{\nu}_{12}$	215	①, ②
alkyl and $\tilde{\nu}_{18a}$	240	①, ②

[a] The transients can be assigned to those modes contributing to these bands.[58] The table lists the beating wavenumbers $\Delta\tilde{\nu}$ observed in the CARS transients of toluene given in Figure 5 (compare refs 35 and 38) and their assignment to the observed bands. A detailed description and visualization of the vibrational modes of toluene is given in ref 46 from where the notation was also taken.

Mode-Selective Excitation under Resonant Conditions. The optimization results presented in Figures 4 and 5 confirm our previous observations[38] and give new insight into the effect of a modulation of the pump laser pulse shape. We have demonstrate that the mode selective excitation under electronically nonresonant conditions is much more efficient if the Stokes laser pulse is shaped by the control algorithm. An efficient control based on a variation of Stokes and pump laser pulse shapes is mainly determined by the phase modulation of the pulses. The stimulated Raman excitation process suggests that the situation should be different if an electronic resonance is involved since here also the dynamics in the excited electronic state will play a role.

In order to investigate the influence of electronic transitions on the optimization process, we have performed a number of experiments on different molecular systems. As a characteristic example, we present results obtained from control experiments on crystal violet (CV) under resonant conditions. The results of the control experiments are presented in Figures 6 and 7. The resulting spectra are shown in the left-hand panels of these figures. The corresponding spectrograms of the pulses obtained from the optimizations are given in the respective panels on

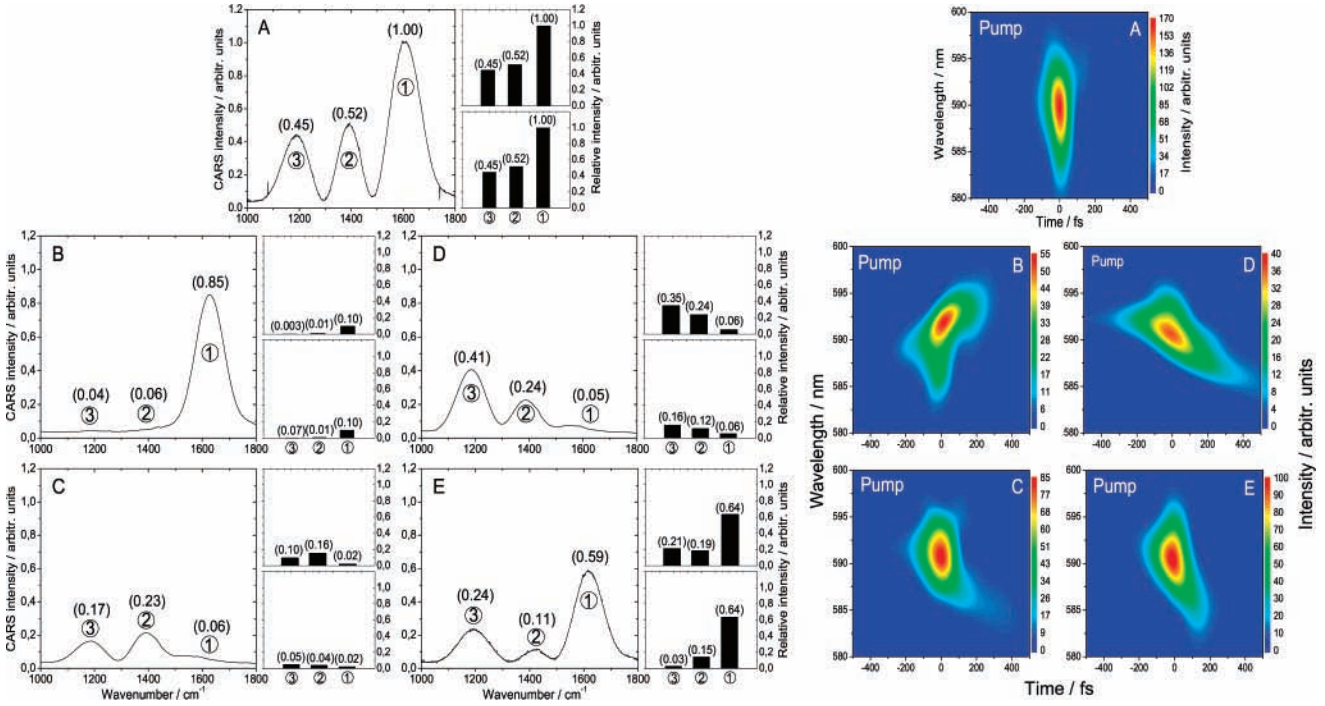

Figure 6. Optimization results in a control experiment on an aqueous solution of crystal violet (CV), where the pure spectral phase of the pump pulse was modulated. The graphs on the left-hand side show the spectra obtained from the optimization, recorded at 900 fs time delay of the probe laser pulse. The numbers in brackets above the different bands indicate their intensities using equal scales for each panel. Panel A shows the spectrum taken with transform-limited pulses for comparison. Panels B−D show the spectra optimized for bands ①, ②, and ③, respectively. Panel E shows the spectrum optimized for a suppression of band ②. The bar diagrams on the right-hand side of the each spectrum show the line intensities predicted from the nonresonant CARS spectrum taken from a thin glass plate (upper diagrams) and obtained from a calculation (bottom diagrams), which used the electric fields of the pulses derived from the FROG traces. The intensity of band ① in panel A is normalized. The corresponding spectrograms are shown in the respective panels A−E on the right-hand side.

the right-hand side. The numbers in the brackets over a certain band in Figures 6 and 7 indicate the ratio of the intensity of these modes relatively to the intensity of band ① given in spectrum A. Spectra A in Figures 6 and 7 are recorded with a transform limited pump pulse. A pure phase modulation of the pulses was used to obtain spectra B−D shown in Figure 6, where a selective excitation of bands ①, ②, and ③ was attempted, respectively. Also without changing the spectral amplitude, drastic changes of the CARS spectra could be achieved by phase modulation similar to the results obtained from electronically nonresonant CARS on toluene and other molecular systems. While the selected vibrational bands ② and ③ are dominating the optimized spectra C and D, respectively, band ① is even exclusively excited in spectrum B as a result of the optimization. Using phase-only modulated pulses we also were able to reduce the intensity of the middle band ② selectively, as shown in panel E of Figure 6.

The results presented in Figure 7 were obtained from control experiments performed including amplitude modulation. The resulting spectra optimized for bands ①, ②, and ③ by means of pure amplitude modulation are shown in panels B−D, respectively. In contrast to the optimization under electronically nonresonant conditions, the pure amplitude modulation of the pump pulse results in drastically changed spectra. However, good optimization results only can be achieved for some of the Raman lines. For CV band ① can be easily varied in intensity while the other bands only can be relatively enhanced when also phase modulation is performed. The spectrum in panel B is characterized not only by a relative but also by an absolute enhancement of the selected band ①. The contributions of bands and are nearly completely suppressed. The selective excitation of bands ② and ③ yields not a full suppression of band ①, but a considerably decreased contribution to the optimized spectra as can be seen from panels C and D, respectively. The intensity ratio of bands ② and ③ cannot be influenced considerably with pure amplitude modulation. Obviously, only the spectral phase change allows for a relative optimization of bands ② and ③. In order to verify this observation, after the amplitude-only modulation we also have admitted fitting parameters influencing the phase of the pump laser pulse. The resulting spectra for an optimization of bands ①, ②, and ③ are shown in panels E−G. Now, a relative and for bands ① and ③ even an absolute enhancement could be achieved. A comparison of the results presented in Figures 6 and 7 reveal the combined modulation of pump pulse as most effective mechanism for selective excitation of vibrational modes under resonant conditions. The comparison of the FROG traces shown in Figure 6 and 7 shows that for the electronically resonant case the amplitude modulation has a considerable influence on the optimization for specific vibrational modes. Without amplitude modulation, no absolute enhancement was achieved. Even higher absolute values are possible if the fitness function used by the evolutionary algorithm also includes an evaluation of the absolute line strengths. Contrary to the electronically nonresonant case, the best results are obtained by a combination of phase and amplitude modulation. A restriction of the spectral width can in the resonant case have advantages. This was already observed earlier for polydiacetylenes. Here, the mode optimization was more efficient, if pulses had a narrower spectrum.

The pulse shapes obtained from the optimization experiments all are considerably changed compared to the initial pulse shown for panels A (right-hand side) of Figures 6 and 7. The pulses obtained from the optimization by means of pure phase modulation shown in Figure 6 are characterized by a strong chirp having considerable nonlinear contributions. The pure amplitude modulation results in a spectral limitation of the

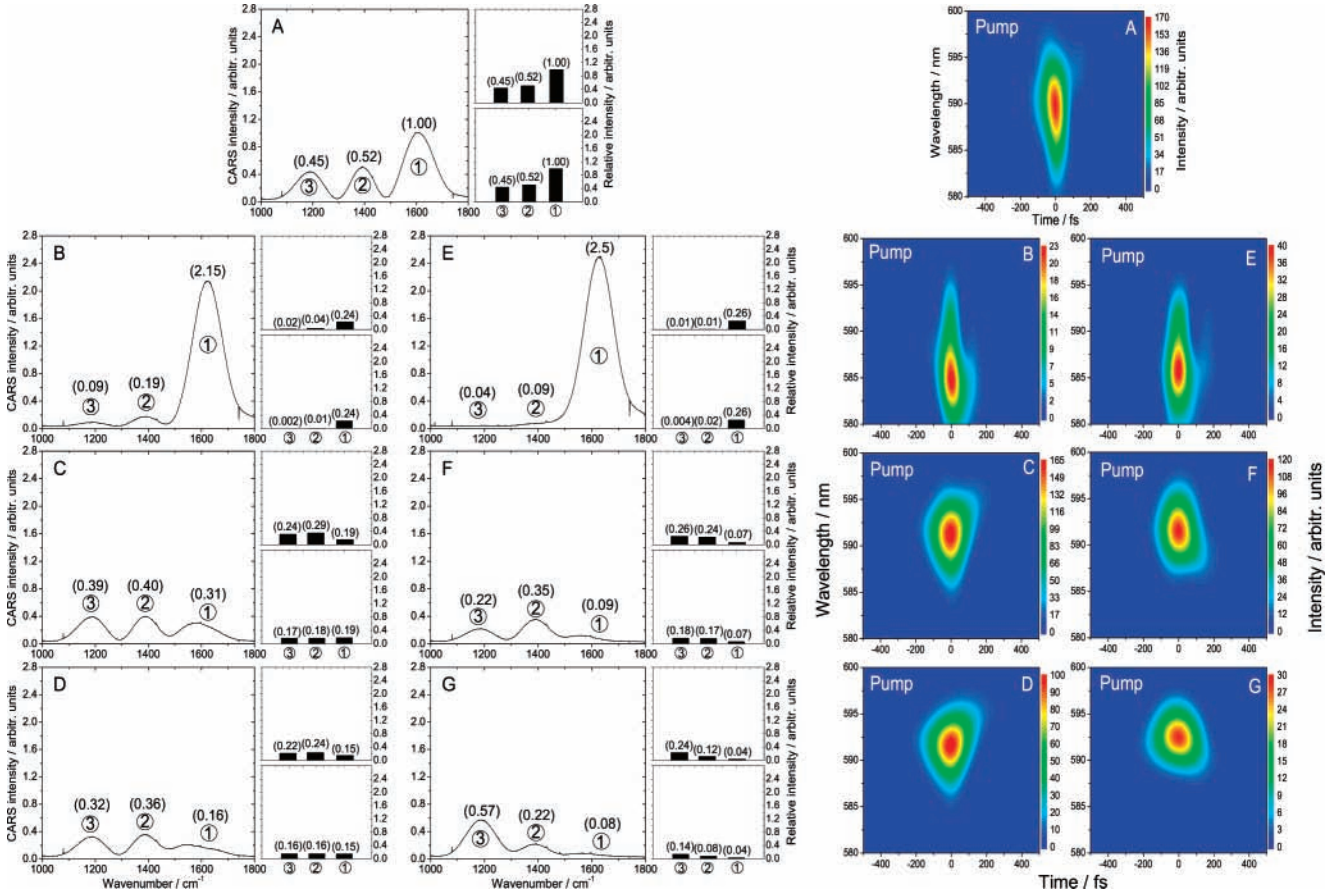

Figure 7. Optimization results in a control experiment on an aqueous solution of crystal violet (CV), where the pure spectral amplitude as well as both the spectral phase and amplitude of the pump pulse were modulated. The graphs on the left-hand side show the spectra obtained from the optimization, recorded at 900 fs time delay of the probe laser pulse. The numbers in brackets above the different bands indicate their intensities using equal scales for each panel. Panels A shows the spectrum taken with transform-limited pulses for comparison. Panels B−D show the spectra optimized for bands ①, ②, and ③ by pure amplitude modulation, respectively. Panels E−G show the spectra optimized for bands ①, ②, and ③ by combined amplitude and phase modulation, respectively. The bar diagrams on the right-hand side of the each spectrum show the line intensities predicted from the nonresonant CARS spectrum taken from a thin glass plate (upper diagrams) and obtained from a calculation (bottom diagrams), which used the electric fields of the pulses derived from the FROG traces. The intensity of band ① in panel A is normalized. The corresponding spectrograms are shown in the respective panels A−G on the right-hand side.

shaped pulse, as seen in the spectrograms displayed in panels B−D of Figure 7. Additionally, the spectral intensity maxima are shifted relative to the original pump laser pulse. The FROG traces of the shaped pulses shown in the spectrograms displayed in panels E−G reflect clearly the contributions of phase as well as amplitude modulation to the control process. The pulses in panels B and E, which result from the optimization of band ① are almost identical. This points to the dominating contribution of the amplitude modulation. In contrast to this, the shapes of the pulses displayed in panels F and G obtained from the optimizations of bands ② and ③, respectively are clearly phase and amplitude modulated. This combined variation of spectral phase and amplitude seems to be required to improve the efficiency of the optimization of these bands.

For electronically nonresonant excitation we have found different mechanisms responsible for the control. If the Stokes laser is shaped, a simple explanation of the control results by means of the ESM or SSM was not possible. There, the predictions made either from the nonresonant measurements on a glass plate nor the calculations using the electric fields of the laser pulses were explaining the CARS spectra.[35,38] Above, we have discussed the results obtained when modulating the pump laser. Here, ESM and SSM are sufficient to predict the band intensities arising from the CARS process initiated by the optimized pulses. In the case of CV (and similar systems like β-carotene or polydiacetylene), the CARS excitation takes place in resonance with an electronic transition of the molecule. Here, ESM and SSM at first sight also play a considerable role.

In Figures 6 and 7 on the right-hand side of each spectrum the predictions based on the experimentally obtained glass spectrum (top) and on the calculation using the light fields (bottom) are given as bar diagrams. Again, the intensity of band ① obtained with transform-limited pulses was normalized, which can be seen in panels A. All other intensities are presented with the same scaling factor. As was described above, also the predicted intensities shown in the bar diagrams were rescaled to fit the intensity of band ① in panels A. The differences between experimental and theoretical predictions are again more pronounced for narrowed pulse spectra. In general, the experimentally obtained nonresonant glass spectra yield better predictions than the calculations. This might have to do with errors introduced by the FROG measurements. A further source of uncertainty is the determination of the exact time zero for the overlap of the laser pulses, which is needed for the calculation of the CARS intensities. However, this value is difficult to determine whether the pulse shapes are not transform limited.

The comparison of the line intensities of the bar diagrams with the line intensities obtained from the CARS experiments after optimization shows that in nearly all cases the qualitative relativ intensity changes are predicted correctly. This points to

the involvement of ESM and SSM in the control process. However, a closer look reveals partially drastic deviations if absolute intensities are taken into account. Striking examples are the spectra obtained for an optimization of band ① (panel B of Figure 6; panels B and E of Figure 7). Here, the predictions of the respective intensity of band ① are wide off the mark. A simple ESM or SSM does not explain the big enhancement factor of this band. This demonstrates the importance of the electronic resonances for the efficiency of the control process. Similar observations were reported by the group of Motzkus.[52,54] They have demonstrated the absolute enhancement of the vibrational motion[54] and selected vibrational modes[52] using multipulse excitation under electronically resonant conditions. The observed absolute enhancement induced by the excitation with periodically phase modulated pulses was explained by the enhanced population transfer to the excited state[54] and by the creation of stronger vibrational coherence.[52] The pulses obtained from the optimization experiments discussed in the present publication do not show any periodic structure in the time domain, which excludes the possibility of the impulsive excitation process by pulse sequences. An other approach to exploit the resonant transition involved in a two-photon process in order to enhance the population of a final state was suggested by Silberberg and co-workers.[55] These authors reported resonant two-photon absorption in rubidium gas. Here, the authors have symmetrically blocked the spectral components of the pulse around the resonance frequency of the intermediate state. This prevents the destructive interference of spectral components around the resonance frequency and results in an absolute enhancement of the fluorescence signal. In contrast to Rb, which is characterized by spectrally narrow transitions to the intermediate state involved in the two-photon process, the absorption of crystal violet is spectrally broad. Therefore, this mechanism can be excluded as well.

As was already pointed out above, the control does not work equally good for all molecular modes and also depends on the molecule under investigation. In our earlier control experiments on polymers of diacetylene we were able to strongly change the intensity ratios for all polymer backbone modes excited by the stimulated excitation process.[34] In the present case, for CV especially band ① can be enhanced or suppressed while the control of the other modes is less efficient. On the one hand the dynamics along the complicated excited potential energy surface will be influenced by the interaction with the shaped laser pulses due to the changed wave packet preparation. On the other hand also the correct timing of pump and Stokes interaction might in the resonant case result in a more favorable Franck−Condon overlap for certain mode excitations. The influence of the excited-state dynamics was already demonstrated previously in CARS experiments on polydiacetylene.[10] Here, a time delay between pump and Stokes laser resulted in drastically changed mode excitations, which could be explained by the ultrafast dynamics along the excited excitonic polymer states. Pinkas et al.[56] improved the Franck−Condon overlap for higher lying overtones in the electronic ground state of iodine by delaying the Stokes interaction. The interaction with the wave packet having propagated along the excited B state during the delay time of the Stokes pulse, allowed for an access to these high-energy vibrational states. Another well-known effect is the focusing of wave packets to certain positions on the potential energy surface after a wave packet preparation with a suitably shaped laser pulse.[57]

Like in the case of the toluene CARS experiments also for CV the changed mode selection survives during the full coherence life time of the signal (not shown here). Since this behavior was observed in all our present as well as earlier experiments, we believe that it is a characteristic feature of this type of control.

Summary and Conclusions

In this contribution we have discussed results obtained from optimal control experiments. By shaping the pump laser of the stimulated Raman excitation process of femtosecond time-resolved coherent anti-Stokes Raman scattering (CARS), the mode excitation is influenced. Guided by an evolutionary algorithm in a feedback-controlled self-learning loop arrangement, specific molecular modes were enhanced or suppressed relative to other contributions in the nonlinear Raman spectrum. We have focused on two new aspects in the spectrum control based on CARS spectroscopy: (i) the investigation of the influence of the pump laser pulse shape on the mode excitation and (ii) the influence of electronic resonances on the control efficiency. All experimental results were compared to the results of earlier experiments where, e.g., the Stokes laser pulse was shaped. Experiments were performed on different molecular systems having absorptions in the visible as well as UV spectral region. As examples we have discussed the outcome of control experiments performed on toluene (electronically nonresonant case) and crystal violet (CV; electronically resonant case).

While for toluene a mode control could be performed very successfully when the Stokes laser was shaped, the pump laser modulation only had a limited influence on the relative mode intensities. While a variation of the spectral phase of the laser pulse was capable of changing the intensity ratios of the different CARS bands, a pure amplitude modulation was not efficient. In contrary, every reduction of the spectral width of the laser pulses resulted in a worse control result. In all cases, the change of intensity ratio resulted in an overall decrease of the absolute line intensities. The situation was found to be different, if an electronic resonance is involved in the CARS process. For CV the pump laser pulse modulation was efficiently changing the relative mode intensities. When varying the amplitudes of the spectral components, even drastic absolute enhancements of specific modes could be detected. The best results were here obtained when both phase and amplitude modulation was optimized by the evolutionary algorithm.

In order to find out whether the control is accomplished by merely shifting the spectral overlap of pump and Stokes laser (phase modulation; "excitation shift mechanism", ESM) or changing the spectral pulse center (amplitude modulation; "spectral selection mechanism", SSM), we have made a prediction of the CARS spectra assuming no contribution from molecular dynamics. For this, the laser pulses after optimization were used to take an electronically and vibrationally nonresonant CARS spectrum from a glass plate. Additionally, we have calculated the expected band intensities using the electric fields of the laser pulses obtained from the FROG traces. While for the pump laser control in toluene the ESM and SSM were the clearly dominating control mechanisms, for the resonant CARS process only the qualitative changes could be related to them. The absolute values of the band intensities cannot be explained by only assuming a change of the excitation frequency window. Earlier time-resolved CARS results on polymers suggest the involvement of excited-state dynamics as well as changes in the Franck−Condon overlap due to wave packet focusing at certain positions of the excited-state potential energy surface as important factor for the mode control.

Acknowledgment. We are very grateful to D. Zeidler and T. Balster for their support in writing parts of the software. Many thanks are due to A. K. Singh (BARC, India) for his support in planning of the experiments and discussion of the results. Spontaneous Raman spectra were provided by M. Sackmann. Fruitful discussions about theoretical aspects of this work with U. Kleinekathöfer are highly acknowledged. We thank the German Science Foundation DFG (Grant MA 1569/10-1,2) for financial support of this project.

References and Notes

(1) Zewail, A. H. *Femtochemistry: Ultrafast Dynamics of the Chemical World*; World Scientific: Singapore, 1994; Vols. I + II.
(2) Manz, J.; Wöste, L., Eds.; *Femtosecond Chemistry*; VCH; Weinheim, Germany, 1995.
(3) Zewail, A. H. *J. Phys. Chem. A* **2000**, *104*, 5660.
(4) Kiefer, W. *J. Raman Spectrosc.* **2000**, *31*, 3.
(5) Leonhardt, R.; Holzapfel, W.; Zinth, W.; Kaiser, W. *Chem. Phys. Lett.* **1987**, *133*, 373.
(6) Materny, A.; Chen, T.; Schmitt, M.; Siebert, T.; Vierheilig, A.; Engel, V.; Kiefer, W. *Appl. Phys. B: Laser Opt.* **2000**, *71*, 299.
(7) Lang, T.; Motzkus, M.; Frey, H. M.; Beaud, P. *J. Chem. Phys.* **2001**, *115*, 5418.
(8) Faeder, J.; Pinkas, I.; Knopp, G.; Prior, Y.; Tannor, D. J. *J. Chem. Phys.* **2001**, *115*, 8440.
(9) Zadoyan, R.; Kohen, D.; Lidar, D. A.; Apkarian, V. A. *Chem. Phys.* **2001**, *266*, 323.
(10) Chen, T.; Vierheilig, A.; Waltner, P.; Heid, M.; Kiefer, W.; Materny, A. *Chem. Phys. Lett.* **2000**, *326*, 375.
(11) Leonhardt, R.; Holzapfel, W.; Zinth, W.; Kaiser, W. *Revue. Phys. Appl.* **1987**, *22*, 1735.
(12) Scully, O. M.; Kattawar, G. W.; Lucht, R. P.; Opatrny, T.; Pilloff, H.; Rebane, A.; Sokolov, A. V.; Zubairy, M. S. *Proc. Natl. Acad. Sci. U.S.A.* **2002**, *99*, 10994.
(13) Tannor, D. J.; Kosloff, R.; Rice, S. A. *J. Chem. Phys.* **1986**, *85*, 5805.
(14) Peirce, A. P.; Dahleh, M.; Rabitz, H. *Phys. Rev. A.* **1988**, *37*, 4950.
(15) Kosloff, R.; Rice, S. A.; Gaspard, P.; Tersigni, S.; Tannor, D. J. *Chem. Phys.* **1989**, *139*, 201.
(16) Judson, R. S.; Rabitz, H. *Phys. Rev. Lett.* **1992**, *68*, 1500.
(17) Warren, W. S.; Rabitz, H.; Dahleh, M. *Science* **1993**, *259*, 1581.
(18) Gordon, R. J.; Rice, S. A. *Annu. Rev. Phys. Chem.* **1997**, *48*, 601.
(19) Rabitz, H.; de Vivie-Riedle, R.; Motzkus, M.; Kampa, K. *Science* **2000**, *288*, 824.
(20) Weiner, A. M. *Rev. Sci. Instrum.* **2000**, *71*, 1929.
(21) Baumert, T.; Brixner, T.; Seyfried, V.; Strehle, M.; Gerber, G. *Appl. Phys. B: Laser Opt.* **1997**, *65*, 779.
(22) Assion, A.; Baumert, T.; Bergt, M.; Brixner, T.; Kiefer, B.; Seyfried, V.; Strehle, M.; Gerber, G. *Science* **1998**, *282*, 919.
(23) Brixner, T.; Damrrauer, N. H.; Gerber, G. *Adv. At., Mol., Opt. Phys. Ser.* **2001**, *46*.
(24) Brixner, T.; Damrrauer, N. H.; Niklaus, P.; Gerber, G. *Nature* **2001**, *414*, 57.
(25) Brixner, T.; Damrrauer, N. H.; Kiefer, B.; Gerber, G. *J. Chem. Phys.* **2003**, *118*, 3692.
(26) Brixner, T.; Gerber, G. *Chem. Phys. Chem.* **2003**, *4*, 418.
(27) Meshulach, D.; Silberberg, Y. *Phys. Rev. A* **1999**, *60*, 1287.
(28) Dudovich, N.; Oron, D.; Silberberg, Y. *Nature* **2002**, *418*, 512.
(29) Oron, D.; Dudovich, N.; Yelin, D.; Silberberg, Y. *Phys. Rev. A* **2002**, *65*, 43408.
(30) Oron, D.; Dudovich, N.; Yelin, D.; Silberberg, Y. *Phys. Rev. Lett.* **2002**, *88*, 063004.
(31) Dudovich, N.; Oron, D.; Silberberg, Y. *J. Chem. Phys.* **2003**, *118*, 9208.
(32) Zeidler, D.; Frey, S.; Kompa, K. L.; Motzkus, M. *Phys. Rev. A* **2001**, *64*, 023420.
(33) Bardeen, C. J.; Yakovlev, V. V.; Wilson, K. R.; Carpenter, S. D.; Weber, P. M.; Warren, W. S. *Chem. Phys. Lett.* **1997**, *280*, 151.
(34) Zeidler, D.; Frey, S.; Wohlleben, W.; Motzkus, M.; Busch, F.; Chen, T.; Kiefer, W.; Materny, A. *J. Chem. Phys.* **2002**, *116*, 5231.
(35) Konradi, J.; Singh, A. K.; Materny, A. *Phys. Chem. Chem. Phys.* **2005**, *7*, 3574.
(36) Konradi, J.; Singh, A. K.; Scaria, A. V.; Materny, A. *J. Raman Spectrosc.* **2006**, *27*, 697.
(37) Konradi, J.; Singh, A. K.; Materny, A. *J. Photochem. Photobiol. A: Chem.* **2006**, *180*, 289.
(38) Konradi, J.; Scaria, A.; Namboodiri, V.; Materny, A. *J. Raman Spectrosc.* **2007**, *38*, 1006.
(39) Mukamel, S. *Principles of Nonlinear Optical Spectroscopy;* Oxford University Press: Oxford, U.K., 1995.
(40) Polack, T.; Oron, D.; Silberberg, Y. *Chem. Phys.* **2005**, *318*, 163.
(41) Weiner, A. M.; Heritage, J. P.; Kirschner, E. M. *J. Opt. Soc. Am. B* **1988**, *5*, 1563.
(42) Stobrawa, G.; Hacker, M.; Feurer, T.; Zeidler, D.; Motzkus, M.; Reichel, F. *Appl. Phys. B: Laser Opt.* **2001**, *72*, 627.
(43) Weiner, A. M. *Prog. Quantum Electron.* **1995**, *19*, 161.
(44) Eckbreth, A. C. *Appl. Phys. Lett.* **1978**, *32*, 421.
(45) Trebino, R.; DeLong, K. W.; Fittinghoff, D. N.; Sweetser, J. N.; Krummbügel, M. A.; Richman, B. A. *Rev. Sci. Instrum.* **1997**, *68*, 3277.
(46) Dollish, F. R.; Fateley, W. G.; Bentley, F. F. *Characteristic Raman Frequencies of Organic Compounds*; Wiley: New York, 1974.
(47) Liang, E. J.; Ye, X. L.; Kiefer, W. *J. Phys. Chem. A* **1997**, *101*, 7330.
(48) Weiner, A. M.; Leaird, D. E.; Wiederrecht, G. P.; Nelson, K. A. *Science* **1990**, *247*, 1317.
(49) Weiner, A. M.; Leaird, D. E.; Wiederrecht, G. P.; Nelson, K. A. *J. Opt. Soc. Am. B* **1991**, *8*, 1264.
(50) Weinacht, T. C.; Bartels, R.; Backus, S.; Bucksbaum, P. H.; Pearson, B.; Geremia, J. M.; Rabitz, H.; Kapteyn, H. C.; Murnane, M. M. *Chem. Phys. Lett.* **2001**, *344*, 333.
(51) Bartels, R. A.; Weinacht, T. C.; Leone, S. R.; Kapteyn, H. C.; Murnane, M. M. *Phys. Rev. Lett.* **2002**, *88*, 033001.
(52) Hauer, J.; H. Skenderovic, K.-L. K.; Motzkus, M. *Chem. Phys. Lett.* **2006**, *421*, 523.
(53) Hellerer, T.; Enejder, A. M. K.; Zumbusch, A. *Appl. Phys. Lett.* **2004**, *85*, 25.
(54) Hauer, J.; Buckup, T.; Motzkus, M. *J. Chem. Phys.* **2006**, *125*, 061101.
(55) Dudovich, N.; Dayan, B.; Gallagher Faeder, S. M.; Silberberg, Y. *Phys. Rev. Lett.* **2001**, *86*, 47.
(56) Pinkas, I.; Knoop, G.; Prior, Y. *J. Chem. Phys.* **2001**, *115*, 236.
(57) Brixner, T.; Pfeifer, T.; Gerber, G.; Wollenhaupt, M.; Baumert, T. In Femtosecond Laser Spectroscopy; Hannaford, P., Ed.; Springer: New York 2005; Chapter 9, page 225.
(58) Chen, T.; Vierheilig, A.; Kiefer, W.; Materny, A. *Phys. Chem. Chem. Phys.* **2001**, *3*, 5408.